

## Modeling Natural Fine Particle Concentrations Using the CMAQ Model with Added Treatments of Reduced Sulfur Compounds

Stephen F. Mueller\* and Jonathan W. Mallard  
Tennessee Valley Authority, Muscle Shoals, AL, USA

### 1. INTRODUCTION

Background levels of fine particles (PM<sub>2.5</sub>) contribute a larger relative share to total PM<sub>2.5</sub> mass as anthropogenic air quality contributions decrease. We have examined natural particle levels using the CMAQ model (version 4.6 with the secondary organic aerosol (SOA) additions used by VISTAS: Morris et al., 2006) by adding reduced sulfur chemistry to both the gas and aqueous chemical components. Gas-phase reactions starting with H<sub>2</sub>S and dimethylsulfide (DMS) were added to the CB05 mechanism. Aqueous-phase reactions involving DMS and its derivatives were incorporated into a new cloud chemistry module. Modeled emissions included contributions from the oceans, soils, wildfires, inland waters, geogenic sources and lightning NO<sub>x</sub>.

### 2. NATURAL EMISSIONS

A natural emissions inventory was developed using the VISTAS 2002 base G inventory (<http://vistas-sesarm.org/>) as the starting point. Anthro-pogenic emissions were removed. Existing soil and biogenic emissions were retained. Development of the natural emissions data base is described in a report being prepared by Shandon Smith (personal communication) who used published emissions factors to estimate sulfur, ammonia and chlorine emissions from a variety of natural surfaces. Sea salt emissions were computed using the method native in CMAQv4.6. No changes were made to the biogenic reactive organic gas emissions in the VISTAS inventory.

Lightning NO<sub>x</sub> (LNO<sub>x</sub>) emissions were derived using a new approach based on established NO<sub>x</sub> emission factors and lightning characteristics (number of strokes, stroke polarity and location) observed by the National Lightning Detection Network (Price et al., 1997; DeCaria et al., 2000; and Thomas Pierce, personal communication). LNO<sub>x</sub> was vertically distributed throughout the modeling domain using a profile developed by Pickering et al. (1998).

\*Corresponding author: Stephen F. Mueller, Tennessee Valley Authority, PO Box 1010, Muscle Shoals, AL 35662-1010; e-mail: [sfmueller@tva.gov](mailto:sfmueller@tva.gov)

Gridded emissions totals for July 2002 are summarized in Table 1 for natural and anthropogenic sources. Overall, natural sources in July 2002 accounted for roughly 44% of the NO<sub>x</sub>, 16% of the gaseous sulfur, 28% of the ammonia, 96% of the total chlorine, and 84% of the primary PM<sub>2.5</sub> emissions within a 5328 km x 4032 km modeling domain covering the continental United States, portions of Canada, Mexico, the Caribbean and adjacent oceans.

**Table 1.** Domain-wide emissions compared for July 2002.

Source & Species	Emissions, Mg
Natural NO <sub>x</sub> <sup>1</sup> .....	9.3x10 <sup>5</sup>
Anthropogenic NO <sub>x</sub> <sup>1</sup> .....	1.2x10 <sup>6</sup>
Natural Sulfur (SO <sub>2</sub> , DMS & H <sub>2</sub> S).....	7.3x10 <sup>4</sup>
Anthro. S (in SO <sub>2</sub> )....	3.7x10 <sup>5</sup>
Natural PM <sub>2.5</sub> .....	1.7x10 <sup>6</sup>
Anthropogenic PM <sub>2.5</sub> .....	3.3x10 <sup>5</sup>
Natural NH <sub>3</sub> .....	1.2x10 <sup>5</sup>
Anthropogenic NH <sub>3</sub> ....	3.1x10 <sup>5</sup>
Natural Cl <sup>2</sup> .....	6.5x10 <sup>5</sup>
Anthropogenic Cl.....	2.7x10 <sup>4</sup>

<sup>1</sup>Expressed as equivalent NO.

<sup>2</sup>Includes chlorine from sea salt, HCl & ClNO<sub>2</sub>.

### 3. MODELING

Meteorological inputs to CMAQ were those produced for the VISTAS regional haze modeling (Abraczinskas et al., 2004). CMAQv4.6 configured with the SOA additions described in Morris et al. (2006) was the base air quality model. Modifications to this configuration are described below.

#### 3.1 Gas-phase Chemical Mechanism

VISTAS used the CMAQv4.6 CBIV chemical mechanism. We opted to use the new CB05 mechanism to take advantage of recent improvements by Yarwood et al. (2005) that influence ozone formation, especially in rural areas in summer. However, several changes were made to the CB05 mechanism to enable simulation of chlorine and reduced sulfur

compounds not treated in the default mechanisms. Several chlorine reactions that are part of an enhanced CBIV mechanism in CMAQv4.6 were moved to CB05. The latter has an enhanced option that includes some chlorine reactions but it also includes organic species that are not relevant to natural emissions modeling. In addition, a number of reactions were added to CB05 to treat oxidation of H<sub>2</sub>S, DMS, and their derivatives. These reactions were added based on NASA (1997), Finlayson-Pitts and Pitts (2000), Tyndall et al. (2001), Kukui et al. (2003), Atkinson et al. (2004), and Zhu et al. (2006). Gas-phase reactions added to CB05 are listed in Tables 2-4.

**Table 2.** Reactions of chlorine species.

---

$\text{Cl}_2 + h\nu \rightarrow 2\text{Cl}$
$\text{HOCl} + h\nu \rightarrow \text{OH} + \text{Cl}$
$\text{PAR} + \text{Cl} \rightarrow \text{HCl} + \text{other organics}$
$\text{OLE} + \text{Cl} \rightarrow \text{other organics}$
$\text{CH}_4 + \text{Cl} \rightarrow \text{HCl} + \text{HCHO} + \text{HO}_2 + \text{XO}_2$
$\text{ETH} + \text{Cl} \rightarrow \text{HO}_2 + \text{HCHO} + \text{other organics}$
$\text{ISOP} + \text{Cl} \rightarrow 0.15\text{HCl} + \text{HO}_2 + \text{other organics}$
$\text{ICL1} + \text{OH} \rightarrow \text{ICL2}$
$\text{O}_3 + \text{Cl} \rightarrow \text{ClO}$
$\text{ClO} + \text{NO} \rightarrow \text{Cl} + \text{NO}_2$
$\text{ClO} + \text{HO}_2 \rightarrow \text{HOCl}$
$\text{ClNO}_2 + \text{OH} \rightarrow \text{HOCl} + \text{NO}_2$

---

**Table 3.** Reactions of H<sub>2</sub>S and derivatives.

---

$\text{H}_2\text{S} + \text{OH} \rightarrow \text{SH} + \text{H}_2\text{O}$
$\text{H}_2\text{S} + \text{NO}_3 \rightarrow \text{SH} + \text{HNO}_3$
$\text{H}_2\text{S} + \text{Cl} \rightarrow \text{SH} + \text{HCl}$
$\text{SH} + \text{O} \rightarrow \text{SO} + \text{H}$
$\text{SH} + \text{O}_3 \rightarrow \text{HSO} + \text{O}_2$
$\text{SH} + \text{NO}_2 \rightarrow \text{HSO} + \text{NO}$
$\text{SH} + \text{Cl}_2 \rightarrow \text{ClSH} + \text{Cl}$
$\text{SH} + \text{NO} + \text{M} \rightarrow \text{HSNO} + \text{M}$
$\text{HSO} + \text{NO}_2 \rightarrow \text{HSO}_2 + \text{NO}$
$\text{HSO} + \text{O}_3 \rightarrow \text{HSO}_2 + \text{O}_2$
$\text{SO} + \text{OH} \rightarrow \text{SO}_2 + \text{H}$
$\text{SO} + \text{NO}_2 \rightarrow \text{SO}_2 + \text{NO}$
$\text{SO} + \text{ClO} \rightarrow \text{SO}_2 + \text{Cl}$
$\text{HSO}_2 + \text{O}_2 \rightarrow \text{HO}_2 + \text{SO}_2$
$\text{CH}_3 + \text{O}_3 \rightarrow \text{CH}_3\text{O} + \text{O}_2$
$\text{CH}_3 + \text{O} \rightarrow \text{CH}_3\text{O}$
$\text{CH}_3\text{O} + \text{O}_2 \rightarrow \text{HCHO} + \text{HO}_2$
$\text{CH}_3\text{O} + \text{NO}_2 \rightarrow \text{HCHO} + \text{HONO}$

---

**Table 4.** Reactions of DMS and derivatives<sup>1</sup>.

---

$\text{DMS} + \text{O} \rightarrow \text{CH}_3\text{SO} + \text{CH}_3$
$\text{DMS} + \text{NO}_3 + \text{O}_2 \rightarrow \text{CH}_3\text{SOOCH}_2 + \text{HNO}_3$
$\text{DMS} + \text{Cl} + \text{O}_2 \rightarrow \text{CH}_3\text{SOOCH}_2 + \text{HCl}$
$\text{DMS} + \text{OH} \rightarrow \text{CH}_3\text{SCH}_2 + \text{H}_2\text{O}$
$\text{DMS} + \text{OH} + \text{O}_2 \rightarrow 0.5\text{DMSO} + 0.2\text{DMSO}_2$ $+ 0.3\text{MSIA}$
$\text{CH}_3\text{SCH}_2 + \text{O}_2 + \text{M} \rightarrow \text{CH}_3\text{SOOCH}_2 + \text{M}$
$\text{CH}_3\text{SCH}_2 + \text{NO}_3 \rightarrow \text{CH}_3\text{SOOCH}_2 + \text{NO}$
$\text{CH}_3\text{SOOCH}_2 + \text{NO} \rightarrow \text{CH}_3\text{S} + \text{HCHO} + \text{NO}_2$
$\text{CH}_3\text{SOOCH}_2 + \text{CH}_3\text{SOOCH}_2 \rightarrow 2\text{CH}_3\text{S} + 2\text{HCHO} + \text{O}_2$
$\text{CH}_3\text{SOOCH}_2 + \text{HO}_2 \rightarrow \text{CH}_3\text{S} + \text{HCHO} + \text{OH} + \text{O}_2$
$\text{CH}_3\text{S} + \text{O}_3 + \text{H}_2\text{O} \rightarrow 0.9\text{SO}_2 + 0.1\text{H}_2\text{SO}_4$
$\text{CH}_3\text{S} + \text{NO}_2 \rightarrow \text{CH}_3\text{SO} + \text{NO}$
$\text{CH}_3\text{SO} + \text{O}_3 \rightarrow 0.14\text{CH}_3\text{S} + 0.86\text{CH}_3$ $+ 0.86\text{SO}_2 + 1.14\text{O}_2$
$\text{CH}_3\text{SO} + \text{NO}_2 \rightarrow \text{CH}_3 + \text{SO}_2 + \text{NO}$
$\text{DMSO} + \text{OH} \rightarrow 0.9\text{MSIA} + 0.1\text{DMSO}_2$
$\text{MSIA} + \text{OH} \rightarrow 0.9\text{SO}_2 + 0.1\text{MSA}$

---

<sup>1</sup>DMSO=dimethylsulfoxide  
DMSO2=dimethylsulfone  
MSIA=methanesulfinic acid  
MSA=methanesulfonic acid

The optimized EBI solver for CB05 cannot be used because of the reaction set modifications. Instead, we used the SMVGEAR solver for our simulations although clearly there is a need for an optimized solver for this modified mechanism.

### 3.2 Cloud Chemistry Module

Organic sulfur compounds are not treated in CMAQv4.6 and the module was modified to accommodate the chemistry of DMS and its derivatives. Based on Zhu (2004), 12 aqueous reactions involving organic sulfur compounds (Table 5) were added to inorganic sulfur chemistry in a new cloud chemistry module. This module maintains the quasi steady-state equilibrium approach currently used in the CMAQ cloud module for assimilating (and, for SO<sub>2</sub>, reacting) species. However, several new species—notably DMSO, DMSO<sub>2</sub>, MSIA and MSA—along with H<sub>2</sub>O<sub>2</sub> are sufficiently reactive that their concentrations in clouds are best treated as transient. The new cloud module solves the set of transient reactions analytically after first computing initial equilibrium concentrations of all dissolved species. In addition, a much shorter time step (1-4 minutes versus the default 6-12 minutes) is used for calling the cloud module to allow for more rapid updating between processes in the gas and cloud phases.

**Table 5.** Aqueous reactions involving organic sulfur compounds and their derivatives.

---

$\text{DMS} + \text{O}_3 \rightarrow \text{DMSO} + \text{O}_2$
$\text{DMS} + \text{OH} \rightarrow \text{DMSO} + \text{HO}_2$
$\text{DMSO} + \text{OH} \rightarrow \text{MSIA} + \text{other products}$
$\text{DMSO} + \text{Cl} \rightarrow \text{CH}_3\text{SO}_2 + \text{other products}$
$\text{DMSO} + \text{SO}_4^- \rightarrow \text{CH}_3\text{SO}_2^- + \text{SO}_4^{2-}$
$\text{DMSO} + \text{Cl}_2^- \rightarrow \text{CH}_3\text{SO}_2^- + \text{other products}$
$\text{DMSO} + \text{O}_3 \rightarrow \text{DMSO}_2 + \text{O}_2$
$\text{DMSO}_2 + \text{OH} \rightarrow 0.3 \text{MSA} + 0.7 \text{SO}_4^{2-}$
$\text{CH}_3\text{SO}_2^- + \text{OH} \rightarrow \text{CH}_3\text{SO}_3^- + \text{H}^+$
$\text{CH}_3\text{SO}_2^- + \text{SO}_4^- \rightarrow \text{CH}_3\text{SO}_3^- + \text{SO}_4^{2-}$
$\text{CH}_3\text{SO}_2^- + \text{Cl}_2^- \rightarrow \text{CH}_3\text{SO}_3^- + 2\text{Cl}^-$
$\text{CH}_3\text{SO}_3^- + \text{OH} \rightarrow \text{SO}_4^{2-}$

---

Tests with the organic chemistry deactivated produce results that are virtually indistinguishable from results with the default CMAQv4.6 cloud chemistry module. Note that the aqueous reaction between DMS and  $\text{O}_3$  is  $\sim 3 \times 10^4$  times faster than the  $\text{SO}_2 + \text{O}_3$  aqueous reaction and  $\sim 2 \times 10^3$  times faster than the  $\text{HSO}_3^- + \text{O}_3$  aqueous reaction at a temperature of 298 K (although the  $\text{SO}_3^{2-} + \text{O}_3$  reaction is twice as fast as the  $\text{DMS} + \text{O}_3$  reaction in water, very little  $\text{SO}_2$  dissociates into  $\text{SO}_3^{2-}$ ).

#### 4. RESULTS

All results described here were obtained from simulating 2002 using the full natural emissions data set without anthropogenic emissions. Model boundary conditions were those used by VISTAS, taken from a global GEOS-Chem air quality simulation (Jacob et al., 2005).

Grid-averaged concentration time series of various particulate species—when coupled with knowledge of emission patterns—reveal much about the behavior of naturally-derived aerosols. Organic carbon (OC) particles dominate the natural  $\text{PM}_{2.5}$  climatology (Figure 1) with summer-time averages across the entire modeling domain peaking above  $1 \mu\text{g m}^{-3}$ . Given the modest SOA formation included in CMAQv4.6, it is likely that even higher levels of OC would be simulated if CMAQ was modified to include aqueous OC formation from isoprene (Ervens et al., 2007) and the new isoprene-epoxide OC mechanism described by Paulot et al. (2009). In summer, EC is second only to OC in abundance across the model grid with averages peaking near  $0.6 \mu\text{g m}^{-3}$ .

Ammonium sulfate (this encompasses total sulfate plus associated ammonium) also peaks in

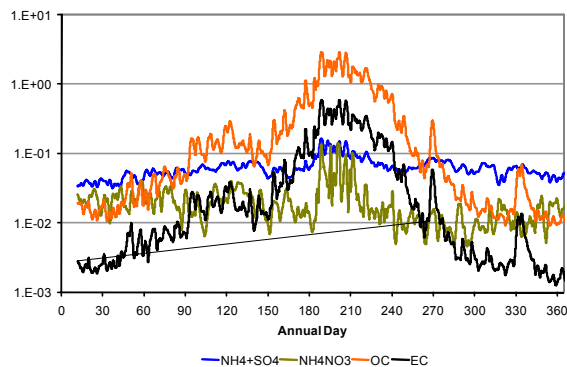


**Figure 1.** Grid-averaged natural fine particle concentration 2002 time series for OC, EC, ammonium nitrate and ammonium+sulfate. Values are  $\mu\text{g m}^{-3}$ .

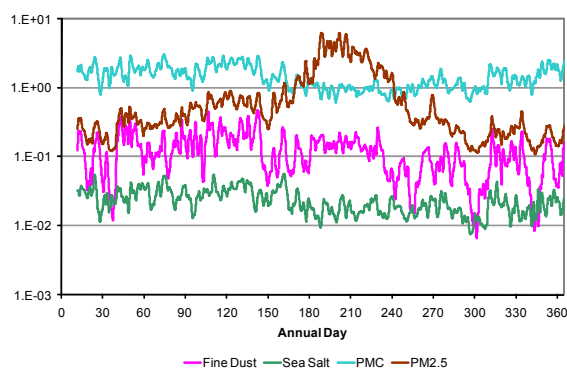


**Figure 2.** Grid-averaged particle concentration 2002 time series for windblown dust ( $<2.5 \mu\text{m}$ ), sea salt ( $<2.5 \mu\text{m}$ ),  $\text{PM}_{2.5}$  and  $\text{PM}_c$ . Values are  $\mu\text{g m}^{-3}$ .

summer, though not as dramatically. Its concentrations rarely exceed those of windblown dust (Figure 2) whose levels are highest in winter and spring. Domain-averaged ammonium nitrate also peaks in summer but decreases by a factor of 10 afterward (Figure 1). Finally, grid-averaged sea salt (Figure 2) is consistently low due to its limited geographic distribution.  $\text{PM}_{2.5}$  mass varies by nearly a factor of 20 from its winter minimum to its summer peak. Coarse particles ( $2.5\text{--}10 \mu\text{m}$ ),  $\text{PM}_c$ , were computed to average mostly  $1\text{--}3 \mu\text{g m}^{-3}$ .

Spatial distributions of simulated natural 2002 maximum 24-h sulfate and OC are illustrated in Figure 3. These plots indicate that patterns of the highest surface particle concentrations are similar. This is because they are primarily emitted by a common, predominant source: wildfires. Numerous fires in 2002 in the western US, Florida and eastern Canada produced the highest modeled sulfate, OC and EC (not shown) concentrations across the domain. For OC, fires easily dominated over SOA formation from biogenic precursor emissions over the southeastern US. However,

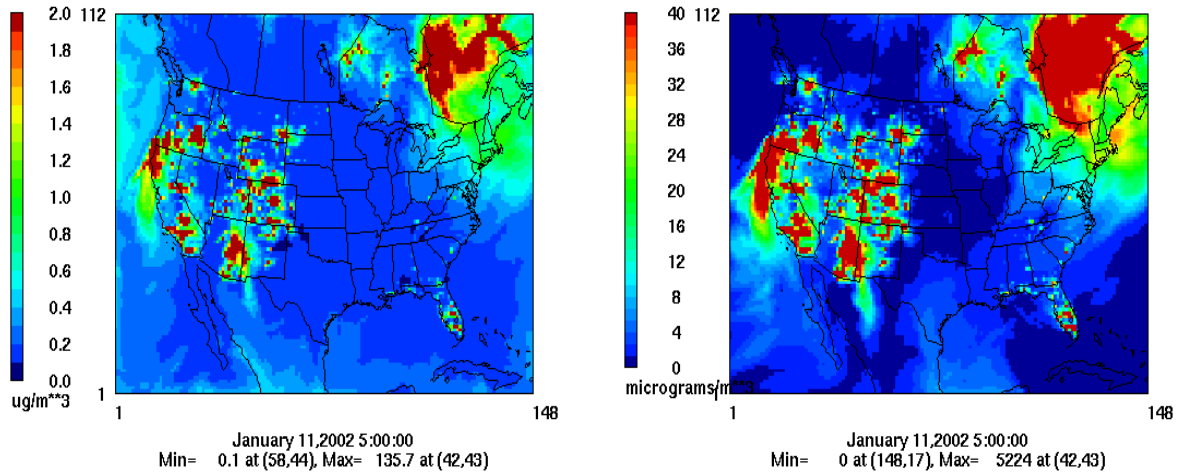


**Figure 3.** Maximum simulated surface layer 24-hr sulfate (left) and organic carbon (right) concentrations for each model grid cell in 2002. For both aerosol types, the hot spots (highest concentrations) are associated with wildfire emissions.

CMAQ has known deficiencies in this area that probably contributed to this outcome.

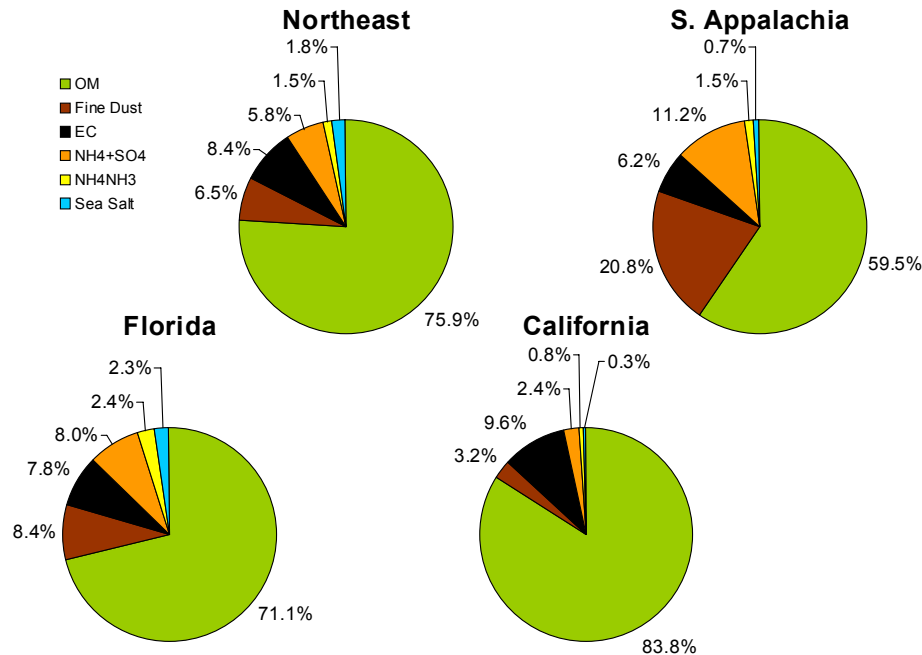
The summer peaks and the spatial plots indicate that wildfires are the predominant source affecting natural  $PM_{2.5}$ . Sulfate, OC and EC levels are each controlled by the spatial and temporal patterns of fires. The stochastic nature of fires suggests large spatial and temporal variability in the particle concentrations associated with them. Windblown dust and sea salt are mostly a wind-driven phenomenon and tend to peak during winter and spring.

Figure 4 illustrates the regional variation in natural  $PM_{2.5}$  composition. Organic  $PM_{2.5}$  called "OM" ( $=1.8 \times OC$ ) dominates everywhere but composes the smallest percentage in Southern Appalachia. This is mostly due to the lower fire activity in this region and not because other components are more abundant. Florida had the highest relative share from ammonium nitrate which seems counterintuitive but is actually tied to the highest annual frequency of lightning in the US.

Much debate within the Regional Planning Organizations has centered on what constitutes natural haze component concentrations. The US Environmental Protection Agency (EPA) issued guidelines for estimating natural visibility that include default values for haze components (EPA, 2003). These guidelines divide the US into "West" and "East" regions. Figure 5 compares simulated natural haze components with the EPA default values for the two US regions in 2002. The model values represent composites of 24-h average concentration distributions for receptors in each region. These composites were obtained by computing the average concentrations of the

annual highest 20 percent of the daily particle distributions at each receptor. Individual site averages were then combined into a single distribution for which the 2.5<sup>th</sup>, 50<sup>th</sup> and 97.5<sup>th</sup> percentiles were calculated. This results in a set of values representing the worst 20 percent days across all regional receptors. Using a single composite distribution composed of all 24-h values for all receptors would have risked biasing the results by clusters of extreme sites. Using all days (rather than the 20 percent highest) would have produced results that were suspiciously clean because many days experienced concentrations so low that values were essentially zero (or background). It also seems inappropriate to use the full range of 2002 meteorological conditions to represent natural background levels for the worst 20 percent of days required under the Regional Haze Rule because the 20 percent worst days are likely those that occurred when meteorological conditions were most favorable for high pollutant loadings (both natural and anthropogenic) in the atmosphere.

The 95 percent confidence intervals of modeled particle concentrations represent the spatial and temporal variability in 24-h simulated values. In most cases (Figure 5) this variability exceeds the factor of 2-3 uncertainty expressed by EPA in its guidance document. Simulated variability for West receptors exceeds one order of magnitude for ammonium sulfate, fine dust and  $PM_c$ , and exceeds a factor of 100 for  $NH_4NO_3$ , OC and EC. Simulated variability is much less in the East, with only OC, EC and  $PM_c$  having confidence intervals exceeding one order of magnitude.



**Figure 4.** Components of natural PM<sub>2.5</sub> averaged for 2002 by region. “Northeast” is comprised of receptors from Maine south to Philadelphia. “S. Appalachia” is comprised of receptors from northern Alabama and Georgia northeast through West Virginia and Virginia. “California” is comprised of receptors from the coast east to the Sierra Nevada Mountains. “Florida” is comprised of receptors throughout the full north-south extent of the state.

CMAQ values are frequently outside the uncertainty bars on the EPA values in Figure 5. This suggests that at the majority of both West and East sites EPA defaults for natural particle concentrations may not represent conditions at the sites. Such disparities were found for NH<sub>4</sub>NO<sub>3</sub>, OC, EC and PM<sub>c</sub> in the West and for EC and PM<sub>c</sub> in the East. Note that EPA defaults indicate higher sulfate in the East than the West whereas the modeling suggests the opposite. This difference is driven by the preponderance of wildfires in the West. Also, CMAQ indicates that OC levels in the West and East are nearly the same whereas the EPA suggests that eastern values should be much higher. The greatest overall disagreement between modeled and EPA-default natural particle levels was found for EC, with CMAQ suggesting that values are more than a factor of 10 greater than indicated by EPA.

## 5. CONCLUSIONS

Natural particle levels simulated by a modified version of CMAQv4.6 produced results that suggest EPA haze component defaults may not represent conditions across the US. EPA-estimated uncertainties are much lower than the variability implied by the modeling, and the

modeled West-East differences in component concentrations were inconsistent with EPA regional haze guidance. The large variability in simulated natural “worst 20 percent” values suggests that using single default concentrations to represent natural background particle levels is not a reasonable assumption. Finally, high 24-h natural concentrations of PM<sub>2.5</sub> indicate that natural conditions are likely to frequently exacerbate attempts to meet fine particle air quality standards. The dominant natural aerosol is clearly the organic component.

## 6. ACKNOWLEDGEMENTS

The Electric Power Research Institute and the Tennessee Valley Authority (TVA) supported this work. We are indebted to Shandon Smith (TVA) for developing the natural emissions data base.

## 7. REFERENCES

Abraczinskas, M.A., D.T. Olerud, and A.P. Sims, 2004: Characterizing annual meteorological modeling performance for visibility improvement strategy modeling in the southeastern U.S., 13th Joint Conf. on Applications of Air Poll. Meteorology, American Meteorological Society.

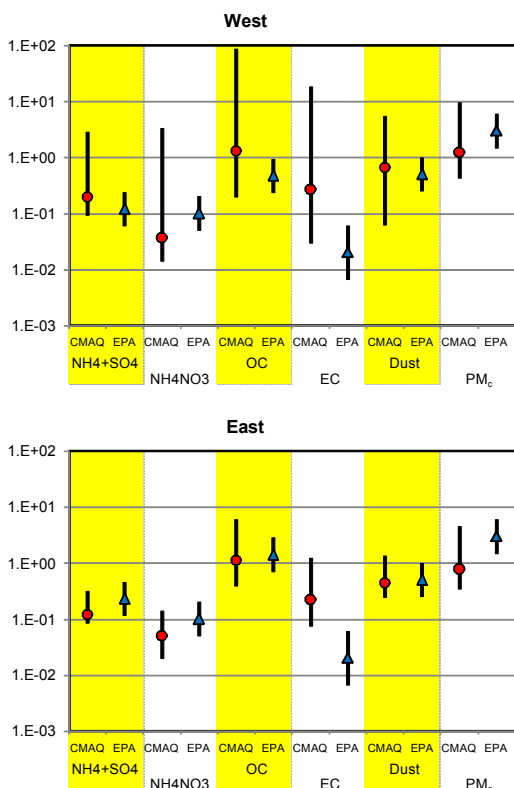


**Figure 5.** Comparison of simulated and EPA default natural haze component concentrations (in  $\mu\text{g m}^{-3}$ ) for 2002 by US region. Red circles denote median model values and blue triangles denote EPA default values. Vertical black lines denote 95 percent confidence interval for simulated values and EPA-estimated uncertainty associated with defaults.

Atkinson, R., and Coauthors, 2004: Evaluated kinetic and photochemical data for atmospheric chemistry: volume I – gas phase reactions of  $\text{O}_x$ ,  $\text{HO}_x$ ,  $\text{NO}_x$  and  $\text{SO}_x$  species, *Atmos. Chem. Phys.*, **4**, 1461–1738.

DeCaria, A.J., K.E. Pickering, G.L. Stenchikov, J.R. Scala, J.L. Stith, J.E. Dye, B.A. Ridley, and P. Laroche, 2000: A cloud-scale model study of lightning-generated  $\text{NO}_x$  in an individual thunderstorm during STEREO-A, *J. Geophys. Res.*, **105**(D9), 11,601-11,616.

EPA, 2003: Guidance for Estimating Natural Visibility Conditions Under the Regional Haze Rule, Office of Air Quality Planning and Standards, Research Triangle Park, NC, EPA-454/B-03-005.

Ervens, B., A.G. Carlton, B.J. Turpin, K.E. Altieri, S.M. Kreidenweis, and G. Feingold, 2007: Secondary organic aerosol yields from cloud-processing of isoprene oxidation products, *Geophys. Res. Lett.*, **35**, L02816, doi:10.1029/2007GL031828.

Finlayson-Pitts and Pitts, 2000: *Chemistry of the Upper and Lower Atmosphere*, Academic Press, San Diego, 328-334.

Jacob, D.J., R. Park, and J.A. Logan, 2005: Documentation and Evaluation of the GEOS-Chem Simulation for 2002 Provided to the VISTAS Group, Harvard University.

Kukui, A., D. Borissenko, G. Laverdet, and G. Le Bras, 2003: Gas-phase reactions of OH radicals with dimethyl sulfoxide and methane sulfonic acid using turbulent flow reactor and chemical ionization mass spectrometry, *J. Phys. Chem. A*, **107**, 5732-5742.

Morris, R.E., and Coauthors, 2006: Model sensitivity evaluation for organic carbon using two multi-pollutant air quality models that simulate regional haze in the southeastern United States, *Atmos. Environ.*, **40**, 4960-4972.

NASA, 1997: Chemical Kinetics and Photochemical Data for Use in Stratospheric Modeling - Evaluation Number 12, Jet Propulsion Laboratory, Publication 97-4, 266 pp.

Paulot, F., J.D. Crouse, H.G. Kjaergaard, A. Kürten, J.M. St. Clair, J.H. Seinfeld, and P.O. Wennberg, 2009: Unexpected epoxide formation in the gas-phase photooxidation of isoprene, *Science*, **325**, 730-733.

Pickering, K.E., Y. Wang, W.-K. Tao, C. Price, and J.-F. Muller, 1998: Vertical distributions of lightning  $\text{NO}_x$  for use in regional and global chemical transport models, *J. Geophys. Res.*, **103**(D23), 31,203-31,216.

Price, C., J. Penner, and M. Prather, M., 1997:  $\text{NO}_x$  from lightning 1. global distribution based on lightning physics, *J. Geophys. Res.*, **102**(D5), 5,929-5,941.

Tyndall, G.S., R.A. Cox, C. Granier, R. Lesclaux, G.K. Moortgat, M.J. Pilling, A.R. Ravishankara, and T.J. Wallington, 2001: Atmospheric chemistry of small organic peroxy radicals, *J. Geophys. Res.*, **106**, 12,157-12,182.

Yarwood, G., S. Rao, M. Yocke, and G. Whitten, 2005: Updates to the Carbon Bond Chemical Mechanism: CB05. Final Report to the US EPA, RT-0400675.

Zhu, L., 2004: *Aqueous Phase Reaction Kinetics of Organic Sulfur Compounds of Atmospheric Interest*, Ph.D. dissertation, School of Earth and Atmospheric Sciences, Georgia Institute of Technology, 261 pp.

Zhu, L., A. Nenes, P.H. Wine, and J.M. Nicovich, 2006: Effects of aqueous organosulfur chemistry on particulate methanesulfonate to non-sea salt sulfate ratios in the marine atmosphere, *J. Geophys. Res.*, **111**, D05316. doi:10.1029/2005JD006326